Current Research in Green and Sustainable Chemistry 8 (2024) 100415

Contents lists available at ScienceDirect

Current Research in Green and Sustainable Chemistry

journal homepage: www.elsevier.com/journals/current-research-in-green-and-sustainable-chemistry/2666-0865

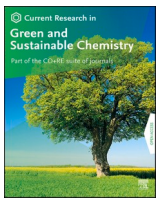

Properties and photocatalytic applications of black TiO_2 produced by thermal or plasma hydrogenation

Manjunath Veeranna Shinnur, MariaPia Pedeferri, Maria Vittoria Diamanti *

Department of Chemistry, Materials and Chemical Engineering, "G. Natta" Politecnico di Milano, Via Mancinelli 7, Milan, 20131, Italy

ARTICLE INFO

Keywords:
Photocatalysis
Black TiO_2
Hydrogenation
Oxygen vacancies
Ti^{3+} species
Pollutants degradation

ABSTRACT

TiO_2 nanomaterial photocatalysts for energy and environmental applications have attracted the interest of researchers in recent decades. The broad bandgap (3–3.2 eV), which limits the quantity of light absorption, and the relatively high charge-carrier recombination, which limits photocatalytic activity, are the key bottlenecks. The discovery of black TiO_2 in 2011 sparked global research attention and renewed optimism for solving this challenge. The presence of defects such as Ti^{3+} species and oxygen vacancies at the surface of black TiO_2 nanostructures – so called due to the color assumed by the oxide following a reduction process - is responsible for enhancing the optical absorption of UV to visible light. This review focuses on recent advancements in the development of black TiO_2 nanomaterials, including description of the synthesis processes, focused on plasma and thermal methods to convert TiO_2 to black TiO_2, discussion of black TiO_2 properties, and diverse applications of black TiO_2, and concludes by addressing some essential concerns that must be tackled to unleash the desired future developments, particularly for solar energy production and pollutants decomposition.

1. Introduction

Heterogeneous photocatalysis has many advantages over traditional water treatment technologies, such as chemical-based procedures, membrane technologies, and adsorption, all of which present issues in treating organic pollutants in wastewater. Similarly, in the face of fossil fuel depletion and growing prices, photocatalysis provides a green and renewable method of producing clean fuel hydrogen by water splitting [1–4]. Researchers are working to produce advanced photocatalytic materials comprising organic molecules, semiconductors, metal complexes, quantum dots, and precious metals. Among these materials, semiconductors have significant advantages over other materials, and are often used in combination with other active materials such as precious metals and quantum dots to improve the overall photo-efficiency [5–7].

Among various semiconductors, TiO_2 has been the most studied photocatalyst due to its chemical stability, earth abundance, low toxicity, thermal stability, and high resistance to photocorrosion [4,8,9]. The use of pure TiO_2 in photocatalysis is restricted in two ways. One is the large band gap (3.2 eV), which hinders most part of solar energy from being absorbed and utilized (only 5 %, i.e., UV radiation). The other is the quick recombination of photogenerated charge carriers, electrons (e^-) and holes (h^+), which significantly diminishes the photocatalytic efficiency [1,10,11]. During past decades, much effort has been dedicated to modify TiO_2 properties to enhance photocatalytic activity and to extend the utilization of solar light to the visible region through metal and non-metal doping techniques [2,12].

However, doping techniques have some drawbacks, such as carrier recombination, thermal instability, and formation of secondary impurities. To overcome these problems, Ti^{3+} self-doping produced by hydrogenation is proposed as an effective technique for modifying pristine TiO_2. In this review, we focus on the latest developments in the synthesis of black hydrogen-treated TiO_2, their properties, and novel attractive applications. Finally, a summary and perspectives on black TiO_2 synthesized through hydrogenation techniques are discussed.

2. Synthesis mechanism

In 2011, it was reported that obtaining a Ti^{3+} defective chemistry changed the electronic band structure of TiO_2 nanocrystals (Fig. 1) by significantly narrowing it for massive visible light absorption and conversion to chemical energy, resulting in significantly improved activity for photocatalytic pollution removal and hydrogen generation from water [13]. Surface, electronic properties, and crystal structures also

* Corresponding author.
E-mail address: mariavittoria.diamanti@polimi.it (M.V. Diamanti).

https://doi.org/10.1016/j.crgsc.2024.100415
Received 13 March 2024; Received in revised form 15 May 2024; Accepted 27 May 2024
Available online 31 May 2024

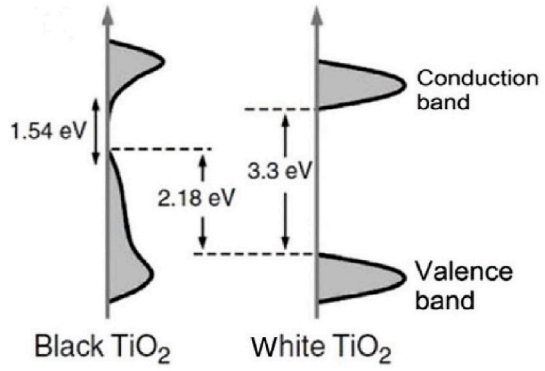

Fig. 1. Schematic illustration of the electronic band structure of black and white TiO_2 nanocrystals. Reprinted with permission from Ref. [13].

undergo significant changes, immediately identified by a change in color – from white to green, yellow, brown, black, and blue [9,12]. Since then, black TiO_2 nanoparticles have sparked a surge in interest in the use of visible light for semiconductor photoactivation.

The synthesis mechanism of black TiO_2 has been studied extensively, with the most widely accepted explanation being that oxygen vacancies (V_O) play a key role in the formation of black TiO_2 [14–16]. These vacancies introduce donor energy levels within the conduction bands. As abovementioned, the creation of V_O is commonly associated with the advent of Ti^{3+}, and both entities contribute to the effective separation of electron–holes pairs generated during photocatalysis [17]. Other effects of hydrogenation include the creation of disordered layers and the formation of Ti– H and O– H bonds beneath the surface. This process also favors the formation of trivalent (Ti^{3+}) and divalent (Ti^{2+}) titanium states. Additionally, it enhances the density of point defects, often resulting in the production of a darker oxide [18,19].

Specifically, when produced by hydrogenation, interactions can be delineated into three steps: firstly, hydrogen physically interacts with the adsorbed oxygen at temperatures below 300 °C. Secondly, when the temperature surpasses 300 °C, electrons are transferred from hydrogen atoms to oxygen atoms in the lattice of TiO_2. Consequently, lattice oxygen is abstracted from the TiO_2 surface, forming H_2O as the oxygen atom departs with the hydrogen atom, resulting in the formation of oxygen vacancies. Thirdly, the interaction between H_2 and TiO_2 intensifies. The electrons from hydrogen atoms are transferred to Ti^{4+} ions in TiO_2, leading to the formation of Ti^{3+} defects [20–22]. Wang et al. [23] revealed that the hydrogenation process induces a shift in the geometric symmetry of TiO_2, leading to structural distortion. This alteration in microstructure is attributed to the generation of V_O following the reduction process, as supported by Electron Paramagnetic Resonance (EPR) analyses, which demonstrated electron trapping at the oxygen vacancies, and (XPS) analyses, confirming the presence of both V_O and Ti^{3+} on the surface of b-TiO_2. Notably, the quantity of oxygen vacancies can be controlled by adjusting the hydrogenation temperature.

Although the capacity of black TiO_2 to utilize visible light has greatly increased, surface defects that generate in the H–TiO_2 surface interaction can be easily oxidized, resulting in a decrease in defect concentration, making black TiO_2 unstable and its applications constrained. Many methods for synthesizing black-TiO_2 nanoparticles have been developed during the last decade, including hydrogenation, plasma treatment, laser ablation, chemical reduction, and electrochemical reduction [2,24,25]; hydrogenation remains the most used approach due to its high efficiency and ease of commercial production [3,26]. While hydrogen thermal and plasma treatments are widely used in photodegradation and solar absorption process, hydrogenation still carries high risk of explosion [27]. In this review, we will focus on these two production techniques, on which a comprehensive review of operational parameters is missing; more details on chemical methods can be found in recent reviews [2,24,28].

3. Synthesis routes

3.1. Hydrogenation

The partial reduction of Ti^{4+} to Ti^{3+}, particularly the reduction of pristine TiO_2, is generally performed by hydrogenation, in which hydrogen (H_2) or mixed atmospheres containing H_2 are utilized as reducing agents [29]. The intrinsic physicochemical properties of pristine TiO_2 nanocrystals (e.g. morphology, size, shape, crystal facet, and defect content), hydrogenation temperature and pressure, and hydrogen time and purity play a vital role in the structure and properties of hydrogenated black TiO_2 nanoparticles [12].

In 1958, D C Cronemeyer found that when rutile TiO_2 single crystals are reduced in a hydrogen atmosphere at temperatures in the order of 600–800 °C for several minutes, followed by cooling the reduced samples in an argon atmosphere, the blue coloration of the crystals is accompanied by high conductivity due to the ionization of trapped electrons in oxygen vacancies. It was found that the blue color arises from the visible tail of infrared absorption band [30].

Chen et al. [13] were then the first research group to synthesize black TiO_2 by hydrogenation of white TiO_2 nanoparticles in a 20 bar H_2 atmosphere at about 200 °C for 5 days. They observed that this hydrogenation process creates a disordered layer on the surface of the TiO_2 nanoparticles, which enhances their solar absorption and photocatalytic activity. They evaluated the solar driven photocatalytic performance of b-TiO_2 by observing the photocatalytic degradation of methylene blue process.

Several works were then published, exploiting different production mechanisms and achieving as a consequence different properties, as listed in Table 1. Earliest attempts involved the use of high pressure (up to 20 bar), temperature and time to achieve hydrogenation, with the latter parameters in countertendency – the lower the temperature selected, the longer the time required to achieve a relevant oxide reduction. Indeed, Wu et al. [31] thermally synthesized black TiO_2 from white TiO_2 through a first step of vacuum degassing at 200 °C for 2 h, followed by heating at 400 °C and treatment with hydrogen in a 5-bar H_2 atmosphere for 24 h. TEM analyses illustrated a disorderly surface layer in b-TiO_2 with a thickness ranging from 4.0 to 8.4 nm (Fig. 2). The synthesized b-TiO_2 exhibited a 53 % higher photocatalytic degradation of tetracycline (TC) under visible light illumination compared to white TiO_2. HR-TEM analyses were also proposed by Zhang et al. [32] who established that as hydrogenation time increased, there was a noticeable disordering in the surface region of the nanoparticles due to reduction-induced defects and lattice rearrangement, highlighting the impact of hydrogenation duration on the structural properties of the TiO_2 nanoparticles.

More recent works aim instead at decreasing process parameters, in order to make the hydrogenation process easier and less energy demanding, also using mixtures of hydrogen and other inert gases – typically nitrogen and argon. Baqaei et al. [22] synthesized hydrogenated TiO_2 nanorods by hydrogenation in a tubular furnace under ambient pressure for 60 min at 400 °C with a gas flow of hydrogen (10 %) and nitrogen (90 %). The prepared photocatalyst exhibited a narrow bandgap of approximately 2.27 eV, showing highly crystalline rutile structure and outstanding photocatalytic properties, as discussed in next sections. Unfortunately, hydrogenation often leads to surface area reduction, as attested by several authors. Wu et al. observed a 50 % reduction, from 41.1 to 22.2 m^2/g, as a consequence of pore loss [31]. A similar result, with 30 % specific area reduction, was observed by Valenzuela et al. [33] and about 95 % drop in the surface area was reported by Rychtowski et al. [19].

An alternative to the hydrogenation treatment consists of obtaining the TiO_2 reduction by annealing in vacuum [48,49] or in nitrogen or

Table 1
Hydrogenation synthesis methods, properties, and photocatalytic applications of the b-TiO_2 materials; performance data report a comparison between the peak efficiency obtained in the best conditions and the reference material (in all cases, pristine TiO_2). Δη is in all cases intended as the percent performance increase with respect to the pristine TiO2 investigated in the same work.

Photocatalyst	Synthesis method	Parameters	Characterization	Performance	Ref.
Black-TiO_2 nanocrystals	Calcination Hydrogen gas atmosphere	Pure H_2 gas T = 200 °C t = 5 days P = 20 bar	Phase: Anatase Morphology: average nanocrystal diameter 8 nm Band gap: 1.54 eV Pristine: 3.30 eV	Target: phenol photodegradation Source: 150 W solar simulator Degradation in 40': 100 % Pristine: 80 % **Δη = +25 %**	[13]
b-TiO_2 nanoparticles	Annealing Hydrogen gas atmosphere	H_2 (99.99 %) T = 600 ÷ 750 °C t = 3 h P = 30 psi	Phase: Anatase Morphology: particle size ~15 nm BET @750 °C: 2.97 m^2/g Pristine: 3.96 m^2/g	Target: methylene blue photodegradation Source: 150 W Xe lamp, 400 nm cutoff filter (VIS) Degradation in 30': 95 % Pristine: 67.89 % **Δη = +40 %**	[33]
b-TiO_2 nanoparticles	Annealing Hydrogen gas atmosphere	H_2 (99.99 %) Flow rate = 1.2 l/min T = 700 ÷ 900 °C t = 1 h P = 1 atm Heating rate = 10 °C/min	Phase: Rutile Morphology: ellipsoidal shape, 92 nm in diameter Band gap: 2.95 eV Pristine: 3.02 eV	Target: rhodamine B photodegradation Source: 300 W Xe lamp; 420 nm cutoff filter (VIS) Degradation in 2 h: 72 % Pristine: <10 % **Δη = +620 %**	[17]
b-TiO_2 nanoparticles	Annealing Hydrogen gas atmosphere	H_2 (99.99 %) T = 400 °C t = 24 h P = 5 bar	Phase: Anatase BET: 22.2 m^2/g Pristine: 41.1 m^2/g Pore size: 16.0 nm Pristine: 15.1 nm	Target: tetracycline photodegradation Source: 1000 W Xe lamp; 400 nm cutoff filter (VIS) Degradation in 270': 66.2 % Pristine: 43.4 % **Δη = +54 %**	[31]
b-TiO_2 nanosheet-assembled microspheres	Annealing Hydrogen gas atmosphere	H_2 (99.99 %) T = 500 ÷ 700 °C t = 3 h P = 1 atm Heating rate = 5 °C/min	Phase: Anatase and rutile Morphology: microsphere, 1 μm diameter BET @600 °C: 82.17 m^2/g Band gap: 2.89 eV	Target: Hydrogen evolution Source: 300 W Xe arc lamp; AM 1.5 filter H_2 evolution rate @600 °C: 4.82 mmol/h/g Pristine: 1.94 mmol/h/g **Δη = +147 %**	[23]
b-TiO_2 particles	Annealing Hydrogen gas atmosphere	H_2 (99.99 %) T = 500 ÷ 700 °C	Phase: Anatase and rutile BET @700 °C: 11 m^2/g Pristine: 215 m^2/g	Target: Hydrogen evolution Source: 150 W Xe lamp; AM 1.5 filter H_2 evolution rate @600 °C after 3 h: 748 μmol/h/g Pristine: 86.4 μmol/h/g **Δη = +760 %**	[19]
b-TiO_2 particles	Annealing Hydrogen gas atmosphere	H_2 Flow rate 50 mL/min T = 500 °C t = 2 h	Phase: Anatase BET: 10 m^2/g	Target: phenol degradation Source: 150 W Xe lamp, 16 W/cm^2 Degradation in 120': 40 % Pristine: 15 % **Δη = +170 %**	[34]
b-TiO_2 particles	Annealing Hydrogen gas atmosphere	H_2 (99.99 %) T = 500 °C t = 5'÷1 h	Phase: Brookite Morphology: nanoparticles, 30 nm diameter	Target: Hydrogen evolution Source: solar simulator AM 1.5 G; 100 mW/cm^2 H_2 evolution rate @ 10': 223 μmol/h/g Pristine: 30 μmol/h/g **Δη = +640 %**	[35]
b-TiO_2 nanotube arrays	Annealing Hydrogen gas atmosphere	H_2 (99.99 %) T = 300 ÷ 500 °C t = 10'÷1 h	Phase: Anatase Morphology: nanotube, length ~4 μm	Target: photocurrent measurements Source: 150 W Xe-lamp Peak IPCE: 52.6 % Pristine: 34.8 % **Δη = +51 %**	[36]
b-TiO_{2-x} nanolaces	Annealing Hydrogen and nitrogen gas atmosphere	Mixture of H_2/N_2 with ratio 1:2 T = 650 °C t = 2 h P = 1 atm	Phase: Anatase and rutile Morphology: nanolace arrays film thickness ~2 μm Band gap @650 °C: 2.21 eV Pristine: 3.41 eV	Target: photocurrent measurements Source: 300 W Xe lamp; 100 mW/cm^2. ABPE: 0.58 %, IPCE @390 nm: 52.51 % Pristine: 0.41 %, 41.89 % **Δη = +25 %**	[37]
b-TiO_2 nanorods	Annealing Hydrogen and nitrogen gas atmosphere	Mixture of 10%H_2/N_2 T = 400 °C	Phase: Anatase and rutile Morphology: nanorods, 90 nm average diameter and 1 μm length	Target: methylene blue photodegradation Source: 300 W Xe lamp; 420 nm	[22]

(*continued on next page*)

Table 1 (*continued*)

Photocatalyst	Synthesis method	Parameters	Characterization	Performance	Ref.
		t = 60 min P = 1 atm Heating rate = 5 °C/min		cutoff filter (VIS) Degradation in 210′: 81.4 % Pristine: 43.8 % **Δη = +86 %**	
b-TiO_2 membranes	Annealing Hydrogen and argon gas atmosphere	Mixture of 5%H_2/Ar Flow rate = 300 sccm T = 600 °C t = 5 ÷ 30 h P = 1 atm	Phase: Anatase Morphology: core-shell ~4 nm thick, defect-rich shell	Target: photodegradation of humic acid Source: UV LED (365 nm); 2.5 mW/cm^2 Degradation in 2 h: 59 % Pristine: 37 % **Δη = +59 %**	[32]
b-TiO_2 nanowire arrays	Annealing Hydrogen and argon gas atmosphere	Mixture of 5%H_2/Ar T = 600 °C t = 6 h P = 1 atm Heating rate = 3 °C/min	Phase: Rutile Morphology: nanowire, diameter ~25.8, length ~3.1 μm	Target: methylene blue photodegradation Source: 500 W Xe lamp; 400 nm cutoff filter (VIS) Degradation rate constant: 0.0275 min^{-1} Pristine: 0.0197 min^{-1} **Δη = +40 %**	[27]
b-TiO_2 nanotube arrays	Annealing Hydrogen and argon gas atmosphere	Mixture of 5%H_2/Ar T = 650 ÷ 850 °C t = 30 min P = 1 atm	Phase: Anatase and rutile Morphology: nanotube, length ~4 μm	Target: water oxidation Source: 450 W Xe lamp; 100 mW/cm^2 Selectivity: 92 % Pristine: 65 % **Δη = +42 %**	[38]
b-TiO_2 nanotube arrays	Annealing Hydrogen and argon gas atmosphere	Mixture of 5%H_2/Ar T = 450 °C t = 1 h	Phase: Anatase Morphology: nanotube, length ~8 μm	Target: phenol degradation Source: solar simulator AM 1.5 G; 100 mW/cm^2 Degradation in 100′: 100 % Pristine: 20 % **Δη = +400 %**	[39]
b-TiO_2 nanoparticles	Hydrogen plasma treatment	H_2 T = 500 °C t = 4 ÷ 8 h Input power = 200 W	Phase: Anatase Morphology: core-shell, ~20 nm in diameter	Target: Hydrogen generation Source: AM 1.5 solar power system H_2 production: 8.2 mmol/h/g Pristine: 0.61 mmol/h/g **Δη = +1200 %**	[40]
Nanoporous b-TiO_2	Hydrogen plasma treatment	Mixture of Ar/H_2 Flow rate = 50 sccm each t = 0 ÷ 120 min Input power = 120 W	Phase: Anatase and brookite Aggregated nanoparticles size @30 min: 20 nm BET @120 min: 427.5 m^2/g Pristine: 18 nm, 62.3 m^2/g	Target: Reactive black B photodegradation Source: 150 W Xe lamp Degradation rate constant: 2 h^{-1} Pristine: 0.39 h^{-1} **Δη = +400 %**	[41]
Mesoporous b-TiO_2 films	Microwave assisted plasma chemical vapor deposition (CVD) system	H_2 Flow rate = 100 sccm t = 5 min P = 5 torr Input power = 300 W	Phase: Mostly amorphous, anatase nanocrystals Morphology: pore size of 8 nm, film thickness 94 nm	Target: photocurrent measurements Source: UV LED (365 nm); 6 mW/cm^2 Current density: 22.9 μA/cm^2 Pristine TiO_2: 0.81 μA/cm^2 **Δη = +2740 %**	[42]
b-TiO_2 nanorods	Inline hot wire chemical vapor deposition (HWCVD) system	H_2 (99.99 %) Flow rate = 200 sccm T_{wire} = 1600 ÷ 1800 °C T_{sample} = 245 ÷ 290 °C t = 20 min P = 2×10^{-7} mbar	Phase: Rutile Morphology: core-shell, shell thickness 2 nm Band gap: 2.9 eV Pristine: 3.0 eV	Target: photocurrent measurements Source: 150 W Xe lamp; 100 mW/cm^2 Current density @390 nm: 1 mA/cm^2 Pristine: 0.25 mA/cm^2 **Δη = +300 %**	[43]
b-TiO_2 films	RF plasma-assisted chemical vapor deposition	H_2 Flow rate = 45 sccm T = 260 °C t = 15 ÷ 60 min P = 13.3 Pa Input power = 200 W	Phase: Anatase Morphology: film thickness @15 min: ~309 nm Pristine: ~342 nm	Target: Methylene blue Source: 15 W UV–vis germicide lamps; 2.2 mW/cm^2 Degradation in 90′: 60 % Pristine: 25 % **Δη = +140 %**	[44]
b-TiO_2 films	Room temperature RF plasma	H_2 Flow rate = 50 sccm T = 25 °C t = 2.5 ÷ 40 min P = 1.5 Pa Input power = 20 W	Phase: Rutile Morphology: micropillar film, 5 μm thickness Band gap: 2.9 eV Pristine: 3.0 eV	Target: photocurrent measurements 50 W Xe lamp; AM 1.5 filter Current density @1.23 V RHE: 2.55 mA/cm^2 Pristine: 0.63 mA/cm^2 **Δη = +300 %**	[45]

(*continued on next page*)

Table 1 (*continued*)

Photocatalyst	Synthesis method	Parameters	Characterization	Performance	Ref.
b-TiO_2 films	AP plasma jet	5 % He/H_2 Flow rate = 200 ml/min Residence time = 0 ÷ 36 s/mm^2 Input power = 10 W	Phase: Anatase Morphology: film thickness 2.5 μm Band gap: 3.29 eV Pristine: 3.34 eV	Target: Photocurrent response Source: UV LED (365 nm); 30 mW cm^{-2} Photocurrent density @24s: 0.8 mA/cm^2 Pristine: 0.15 mA/cm^2 **Δη = +430 %**	[46]
b-TiO_2 nanotubes	DC plasma treatment – comparison with annealing	Mixture of Ar/H_2 T = 25 °C t = 1 h P = 10^{-3} Torr Input power = 5 ÷ 45 W	Phase: Anatase Morphology: nanotubes, average diameter 150 nm, tube length of 9 μm Band gap: ~3.0 eV Pristine: 3.2 eV	Target: Hydrogen production Source: UV LED (365 nm); 80 mW/cm^2 H_2 evolution rate @15 W: 6.6 μL/h/cm^2 Pristine: 1.3 μL/h/cm^2 **Δη = +400 %**	[47]

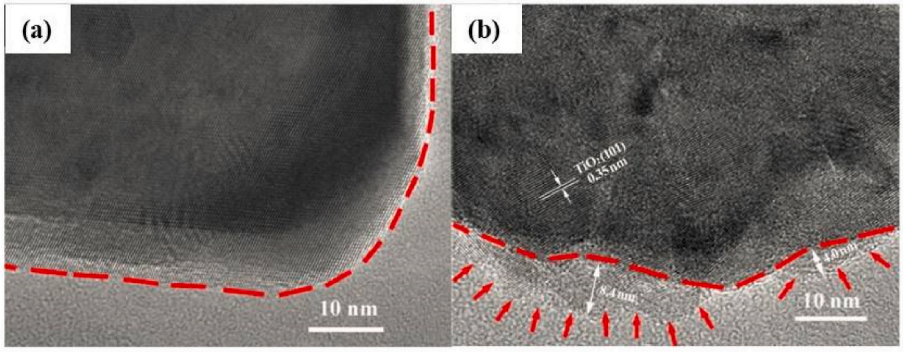

Fig. 2. TEM images of (a) W–TiO_2 and (b) b-TiO_2. Reprinted with permission from Ref. [31].

argon atmospheres, typically at temperatures between 300 and 500 °C for 1 or 2 h [50–54]: this also forces the oxide to reduce, and create the vacancies that are responsible for its enhanced optical properties. Interestingly, Chen et al. (2023) proposed the combination of vacuum annealing and sintering, in order to combine the production of a highly photoactive black TiO_2 ceramic from a TiO_2-based green body: in this work, the sintering phase is performed in vacuum to promote not only sintering itself, but also conversion to b-TiO_2. Since literature mostly deals with free nanopowders, this work sheds some light on more concrete applications of the technology [55,56].

3.2. Plasma

Black TiO_2 can also be produced by plasma treatments. An overview of works where plasma is used for TiO_2 reduction is also contained in the second part of Table 1.

Wang et al. [40] were the first one to use this method to synthesize plasma-reduced black titania. Similarly, in 2016, An et al. [41] prepared hydrogenated nanoporous TiO_2, featuring a substantially large surface area of 427.5 m^2/g, through hydrogen plasma technique. The process involved the use of Ar gas (50 sccm) as carrier gas and H_2 gas (50 sccm) as reactive gas. The treatment time ranged from 0 to 120 min, with a plasma power of 120 W. The H_2 plasma system not only led to hydrogenation, but also to the creation of a porous structure in TiO_2, and simultaneously ensured oxide crystallization, removing the need for further annealing. The increased porosity achieved in this work provided a large number of active sites, resulting in improved photocatalytic performance towards the degradation of organic compounds (phenol, reactive black, rhodamine B and methylene blue).

Godoy-Junior et al. [44] also utilized plasma technique, but in this case a radio-frequency plasma-assisted chemical vapor deposition (RF-CVD) system with a hollow cathode design was employed. The study focused on the effect of the duration of hollow cathode hydrogen plasma treatment on the resulting black TiO_2 films, and concluded that it was able to introduce in-bandgap states in the TiO_2 structure, leading to increased light absorption and enhanced conductivity. They also observed the creation of disorder in the anatase structure already mentioned by Wu et al. [31] as confirmed by a shift in XRD peaks.

Interestingly, Khorashadizade et al. [47] reported the comparative study on black-TiO_2 nanotubes (b-TNTs) synthesized via thermal hydrogenation and plasma treatment. Black-TiO_2 nanotubes were fabricated via thermal hydrogenation in a tubular furnace at different temperatures under a mixed Ar/H_2 (90/10 vol %) atmosphere for 1 h. Black-TiO_2 nanotubes were fabricated via plasma treatment involving mixed Ar/H_2 (90/10 vol %) DC plasma treatment in an ultrahigh vacuum (UHV) chamber with a base pressure of 10^{-8} Torr, and the reduction was carried out at a pressure of 10^{-3} Torr at ambient temperature for 1 h with different applied powers. According to photoelectrochemical analyses, plasma-treated black TiO_2 nanotubes exhibited significantly higher charge carrier density caused by surface defects, and correspondingly higher hydrogen production rate, compared with thermally hydrogenated samples. A similar comparison was conducted by Zhang et al. [57], who compared RF atmospheric pressure plasma and thermal hydrogenation in pure H_2 or He/H_2 mixture, indicating the superior presence of active species in plasma-treated materials, although performances were not tested. It should be noted that the work aimed at identifying the differences between the two processes in similar working conditions, which strongly disadvantaged thermal hydrogenation due to the long process time required as compared with plasma (hours vs minutes). Indeed, plasma treatments are key to reduce the harshness of the process by limiting treatment temperature and duration. This is shown also in the work by Wang et al. [45], where hydrogenation is achieved in few minutes at room temperature and low RF power, leading to a 300 % increase in photocurrent production, as well as in that by Sener et al. [46], who achieved a 200 % improvement in photocurrent density with a residence time of only 20 s per millimeter of treated area at a power of

10 W.

3.3. Stability

As discussed earlier, one of the major problems with black TiO_2 is its stability, which limits its applications. In 2015, Nandasiri et al. [58] conducted a systematic study on the thermal stability of hydrogenated-TiO_2 using nuclear reaction analysis. The findings unveiled the constrained stability of H–TiO_2, primarily attributed to the diffusion of hydrogen into interfaces, subsequently leading to desorption in the form of H_2O, H_2, and surface reduction. Liu et al. [59] investigated the synergistic effects resulting from the combination of electrochemical cathodic reduction and high-pressure hydrogenation treatment techniques. Their experimental findings indicated that when the hydrogenated samples were exposed to air for one day, there was a significant decrease in its photoactivity, confirming its low stability. Indeed, this is related with the generation of Ti^{3+} defects at the material surface rather than in its volume, as the surface is where the contact with the hydrogen flow takes place. To obtain stability improvement, volume Ti^{3+} generation is required. In this direction, Gao et al. [17] prepared black TiO_2 nanoparticles through ultrafast hydrogen flow at a constant heat rate of 10 °C/min. The samples were then held at different temperatures (700–900 °C) for 1 h. Several characterization methods revealed good surface crystallization of the obtained black-TiO_2 with a large amount of oxygen vacancies and a high concentration of internal defects rather than surface defects, which increased the stability of black TiO_2.

4. Optical properties

The presence of defects and/or surface disorder leads to alterations in the electrical and optical properties of black TiO_2. The narrowing of the bandgap serves as a clear indication of the shift in the material band structure. As already discussed, many reports suggest that Ti^{3+} species within the bulk of TiO_2 are responsible for bandgap narrowing. Additionally, the presence of mid-gap states due to oxygen vacancies further intensifies light absorption for photon energies below the direct bandgap through indirect electron transitions.

Zyabkin et al. [60] studied the effects of hydrogenation on the UV–visible absorption spectra of the b-TiO_2 films obtained from H_2 plasma treatment (plasma-CVD system). The impact of hydrogenation is noticeable at low and high temperatures. Hydrogenation of TiO_2 results in a significant increase in absorbance, a characteristic response indicating the influence of oxygen vacancies on light absorption properties b-TiO_2 films. Moreover, the sample hydrogenated at room temperature resulted in a slight reduction in optical band gap of 0.04 eV, while the sample treated at high temperature (300 °C) exhibited a more substantial reduction in band gap of 0.13 eV. In other studies, wider modifications were successfully attained, as demonstrated by Huh et al. [61] where the band gaps of TiO_2 and b-TiO_2 were determined to be 3.16 and 2.62 eV, respectively (Fig. 3). The more effective reduction in the band gap is attributed to the utilization of a simple, room temperature atmospheric pressure plasma jet (APPJ) treatment technique. This method offers superior control over defect formation, crystallinity, and surface wettability, resulting in enhanced optical properties compared to b-TiO_2 synthesized using the plasma-CVD system.

In studies related to black-TiO_2 prepared via the thermal hydrogenation technique, Chahrour et al. [37] observed a reduction in the band gap from 3.39 to 2.21 eV. Similarly, Echeverrigaray et al. [18] reported a 0.3 eV blue shift in bandgap energies from UV–Vis spectra. This shift was attributed to a synergistic interaction between carriers and impurities, specifically V_O and trapped electrons due to Ti^{3+} species, leading to sub-gap absorption.

5. Electrical properties

The electrical properties of TiO_2, including parameters like electrical conductivity and the mobility of charge carriers, exhibit high sensitivity to surface defect disorder. Therefore, numerous studies have demonstrated that hydrogenation of crystalline TiO_2 leads to a notably improved charge transfer process [1,3]. In the following, the works referring to black TiO_2 electrical properties are discussed.

As a starting point, Huh et al. [61] conducted an evaluation of the electrical properties of the b-TiO_2 synthesized by room temperature atmospheric pressure plasma jet in comparison to commercially available TiO_2 via four-point probe. The electrical conductivity of b-TiO_2 was nearly three times higher than that of TiO_2 across all measurement conditions. Even more, Godoy-Junior et al. [44] demonstrated that b-TiO_2 synthesized under 60 min of hollow cathode hydrogen plasma (HCHP) treatment leads to a remarkable enhancement in its electrical conductivity by 99.98 % (Fig. 4b). These enhancements in conductivity can be attributed to the increased concentration of Ti suboxides ($Ti^{3+}/^{2+}$) in the black TiO_2 thin films (Fig. 4a), which lead to an excess of electrons in the electronic states adjacent to the Fermi edge, as also observed by Baqaei et al. [22].

In a more detailed study, Lui et al. [62] evaluated the effects of mechanical pressure and temperature on the electrical conductivity of hydrogenated b-TiO_2. The complex variation in resistivity of black titania under pressure is attributed to changes in carrier concentrations caused by alterations in the band gaps of involved Ti–O phases during compression. Specifically, higher pressure resulted in a larger band gap, leading to higher electrical resistivity. It was found that there is a substantial improvement in electrical transport, 2 to 3 orders of magnitude, in TiO_2 hydrogenated at 800 °C compared to that hydrogenated at 500 °C under high pressures. This improvement was attributed to the higher degree of hydrogenation, controlled by temperature, which led to the formation of the Ti_9O_{17} Magnéli phase.

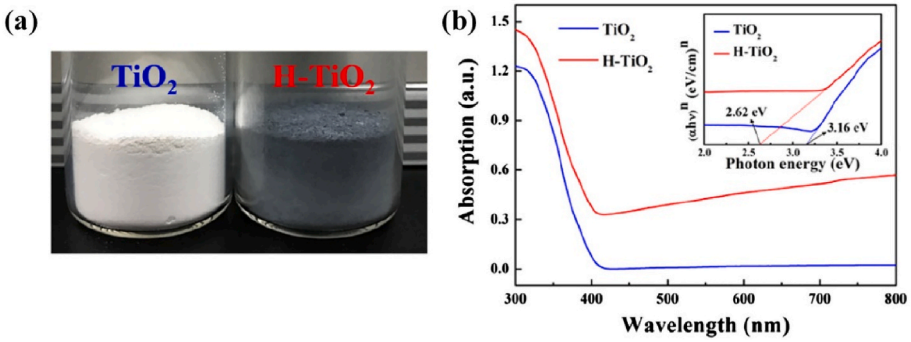

Fig. 3. (a) Photographs and (b) UV–vis absorption spectra (the inset shows the corresponding Tauc plots for the measured band gap) of TiO_2 and as-synthesized H–TiO_2. Reprinted with permission from Ref. [61].

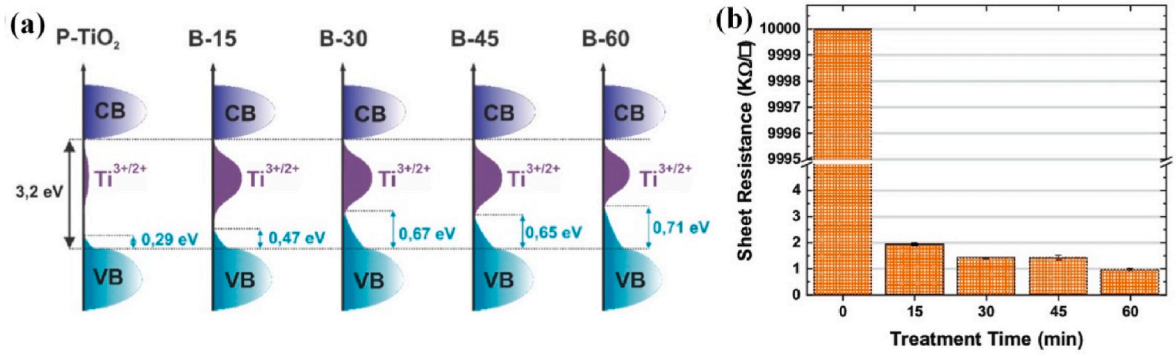

Fig. 4. (a) Schematic representation of defects $Ti^{3+}/^{2+}$ and (b) sheet resistance (in kΩ per square-□) as a function of HCHP treatment time. Reprinted with permission from Ref. [44]. Copyright 2023, MDPI.

6. Photocatalytic application of black TiO_2

Defective TiO_2 exhibits promising attributes in diverse photocatalytic applications, ranging from environmental remediation to hydrogen production through water splitting, and extend to various electrochemical applications, operating as a photoelectrode for batteries and supercapacitors [63,64].

As mentioned in previous sections, Baqaei et al. [22] synthesized H-TNRs and tested them for the degradation of organic compounds in aqueous solutions. They demonstrated 81.4 % degradation of MB in water under 210 min of visible light irradiation.

The experimental results by Godoy-Junior et al. [44] confirm the enhanced photocatalytic efficiency of the HCHP hydrogenated samples, which successfully removed over 45 % of MB dye within just 90 min of UV light exposure, compared to the untreated film roughly 25 % degradation.

Concerning treatment parameters, according to Gao et al. [17] H_2 treatment at 800 °C gave the highest performance with respect to lower hydrogenation temperatures. A series of stability experiments was also conducted on 800 °C–H–TiO_2, including a natural aging treatment lasted 18 months in an air atmosphere. Remarkably, the material retained its characteristic black appearance and its photodegradation efficiency was only 10.5 % lower than that of the freshly hydrogenated samples, indicating a high degree of stability in this black TiO_2 material. Further aging tests were conducted dispersing it in aqueous solutions with varying pH levels, adjusted using HCl or NaOH. Long-term immersion in acid solution even improved the material photocatalytic activity due to changes in surface states induced by protonation. Conversely, after 180 h immersion in alkaline solution with pH 10 ÷ 12, H–TiO_2 demonstrated slightly reduced photocatalytic performance, but still retained nearly 80 % residual efficiency. This study highlights the quality and adaptability of the synthesized black TiO_2 material in different environmental conditions.

As previously mentioned, Zhang et al. [32] developed hydrogenated TiO_2 membranes with improved photocatalytic and anti-fouling properties for ultrafiltration of surface water. The research demonstrated a direct correlation between the hydrogenation time of TiO_2 and the rate of degradation of humic acid under UV light irradiation, with highest performance achieved after 30 h hydrogenation getting 60 % more efficiency compared with pristine TiO_2 (Fig. 5). The impact of plasma power factor on the photoelectrochemical performance of plasma-reduced TiO_2 was studied by Khorashadizade et al. [47]. According to their analysis, photoelectrochemical measurements indicated that the IPCE value, initially at 11 % for the pristine TNTs photoelectrode, underwent a significant increase to 38 %, 60 %, and 46 % for the b-TNTs produced at 5 W, 15 W and 45 W, respectively.

The mechanism of photocatalytic activity enhancement is well explained in several experimental works. Chahrour et al. [37] demonstrated enhanced efficiency of b-TiO_{2-x} nanolace films in the photocatalytic reduction of Cr(VI), which was attributed to self-doping of Ti^{3+} induced by hydrogen reduction and consequent decrease in band gap energy, thanks to the formation of a mid-gap energy level, which significantly enhances the reduction activity. The presence of doped Ti^{3+} on the surface serves as an effective electron trap, thereby suppressing the recombination of electron-hole pairs. Zou et al. [65] also reported a photocatalytic hydrogen evolution rate ten times higher in TiO_2 hydrogenated at 700 °C than that of untreated TiO_2. The significant improvement photocatalytic performance was ascribed to the hydrogenation-induced oxygen vacancies on the surface of TiO_2 and the reduction of bulk defects, which benefits the transfer and the separation of e^- –h^+ pairs.

Analogously, Xu et al. [38] demonstrated that morphology changes and substoichiometric phases, including TiO, Ti_2O_3, and Ti_4O_7, led to enhanced photocurrent density and energy conversion efficiency.

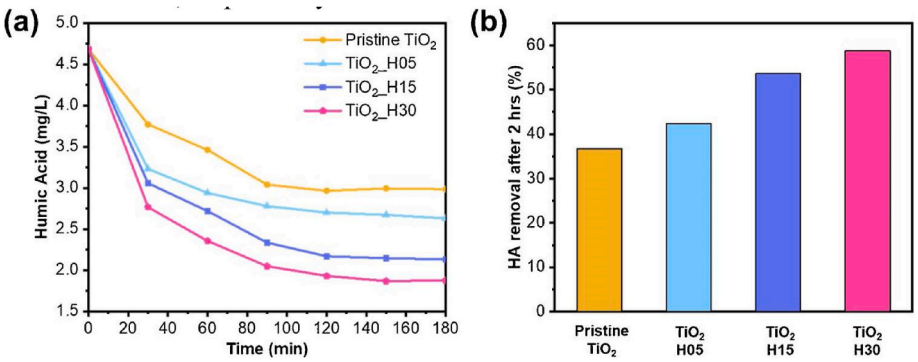

Fig. 5. Photocatalytic performance (a) UV-assisted photocatalytic degradation of humic acid. (b) Humic acid removal by TiO_2 membranes with various hydrogenation duration, compared after 2 h of UV irradiation. Reprinted with permission from Ref. [32].

Specifically, hydrogenated TiO_2 NTs annealed at 800 °C showed a 2.5-fold increase in photocurrent at 1.5 V_{RHE} (Fig. 6d) and a 2.8-fold increase in photoconversion efficiency under solar illumination compared to pristine ones. This improvement was attributed to the increased density of states at the surface, as measured by Electrochemical Impedance Spectroscopy (EIS) (Fig. 6a-c), as well as a reduction in interfacial recombination processes.

Similar studies were conducted on hydrogenated TiO_2 modified with Au nanoparticles by Wang et al. [66]. Photocurrent measurements indicated a modest activity in Au-modified TiO_2, which contrasted with the better results obtained on Au/H–TiO_2 under both UV and visible light illumination.

Wang and Chou [27] conducted a comparative study investigating the effects of thermal treatment and plasma treatment on the formation and photocatalytic activities of black TiO_2 nanowires. Photocatalytic measurements, based on the degradation of methylene blue, revealed that thermally reduced black TiO_2 nanowires exhibited an activity almost 1.25 times higher than that of plasma-reduced black TiO_2 nanowires. Moreover, photoelectrochemical measurements indicated that water splitting efficiency versus pristine nanowires was enhanced by a factor of 57 after thermal treatment, whereas by only 13 for plasma treatment. These findings differ from those of Khorashadizade et al. [47] who found plasma-treated samples exhibited significantly higher photocatalytic performance than thermally treated samples. The variations observed in the outcomes of these studies signify the complex nature of these treatment techniques and highlights the importance of keeping track of the specific production conditions and parameters to understand the real effectiveness of the different treatments, in the view of a future application.

7. Summary and perspective

Over the last decade, numerous studies have focused on synthesizing and explaining different properties of black TiO_2 to improve its performance as a photocatalyst under visible irradiation. The conventional method for preparing black TiO_2 involves a high-pressure hydrogen atmosphere (20 bar) at 300 °C for 5 days, which is complex and not cost-effective for practical applications. Consequently, various alternative synthesis methods for black TiO_2 have been explored, especially plasma treatment.

Hydrogen thermal treatment induces defects such as oxygen vacancies or Ti^{3+} interstitial sites in both the bulk and surface of the material. During thermal annealing, bulk defects tend to migrate towards the surface, leading to enhanced surface defects and improved photocatalytic activity. These alterations introduce midgap states or narrow the band gap. Additionally, the presence of oxygen vacancies in black TiO_2 leads to an increase in donor density, resulting in improved electrical conductivity, charge transport and separation of photoexcited charges within the material. Yet, surface defects are unstable, and the improvement in photoactivity can easily be lost by simple exposure to atmospheric conditions. The stability aspect is one of the major concerns in this research field, and still need solutions to enhance also bulk defect production.

The extent of defects production, and whether they have a positive or negative impact on the material properties, relies on the synthesis conditions. It is crucial to carefully regulate the hydrogenation process, considering factors such as pressure, temperature, and duration; under unsuitable processing conditions, the formed structural defects may act as charge recombination centers, resulting in lower photocatalytic efficiency.

The practical application of black TiO_2 faces significant challenges due to the extreme hydrogenation conditions, including high temperature, pressure, and prolonged treatment time. This poses a significant challenge in developing a simple and cost-effective method for preparing highly stable black TiO_2. Therefore, there is a need for novel hydrogenation methods that offer highly efficient, mild treatment conditions, and scalability in fabrication. These would enable the synthesis of black TiO_2 with superior properties suitable for practical photocatalytic applications.

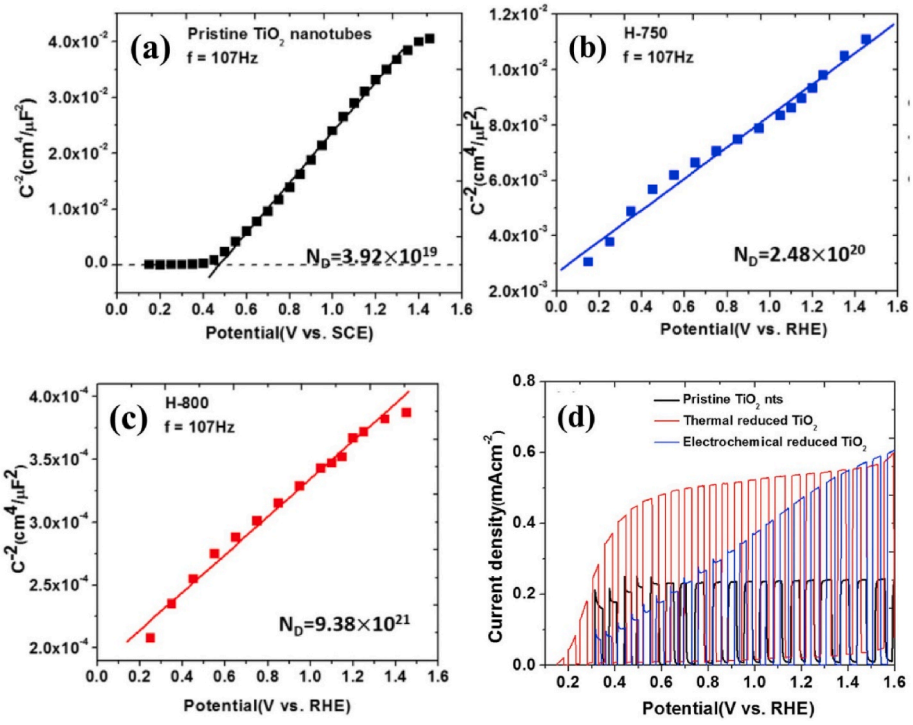

Fig. 6. Mott-Schottky plots and calculated density of donors for (a) pristine TiO_2, (b) H-750, (c) H-800 measured by EIS and (d) linear sweep voltammograms of pristine TiO_2 NTs, thermal reduced Ti–O compounds and electrochemically reduced TiO_2 NTs. Adapted with permission from Ref. [38].

Declaration of competing interest

The authors declare that they have no known competing financial interests or personal relationships that could have appeared to influence the work reported in this paper.

Data availability

The data used in this work are taken from literature works. No new data was published.

Acknowledgement

This study was carried out within the MICS (Made in Italy —Circular and Sustainable) Extended Partnership and received funding from the European Union Next–Generation EU (PIANO NAZIONALE DI RIPRESA E RESILIENZA (PNRR) MISSIONE 4 COMPONENTE 2, INVESTIMENTO 1.3 —D.D 1551.11-10-2022, PE00000004).

References

[1] X. Yan, Y. Li, T. Xia, et al., Black titanium dioxide nanomaterials in photocatalysis, Int. J. Photoenergy 2017 (2017).
[2] S.G. Ullattil, S.B. Narendranath, S.C. Pillai, P. Periyat, Black TiO2 nanomaterials: a review of recent advances, Chem. Eng. J. 343 (2018) 708–736.
[3] T. Rajaraman, S.P. Parikh, V.G. Gandhi, Black TiO2: a review of its properties and conflicting trends, Chem. Eng. J. 389 (2020) 123918.
[4] Z. Li, S. Wang, J. Wu, W. Zhou, Recent progress in defective TiO2 photocatalysts for energy and environmental applications, Renew. Sustain. Energy Rev. 156 (2022) 111980.
[5] A.L. Linsebigler, G. Lu, J.T. Yates Jr., Photocatalysis on TiO2 surfaces: principles, mechanisms, and selected results, Chem. Rev. 95 (3) (1995) 735–758.
[6] X. Chen, S.S. Mao, Titanium dioxide nanomaterials: synthesis, properties, modifications, and applications, Chem. Rev. 107 (7) (2007) 2891–2959.
[7] Z. Xiu, M. Guo, T. Zhao, K. Pan, Z. Xing, Z. Li, W. Zhou, Recent advances in Ti3+ self-doped nanostructured TiO2 visible light photocatalysts for environmental and energy applications, Chem. Eng. J. 382 (2020) 123011.
[8] S. Selcuk, X. Zhao, A. Selloni, Structural evolution of titanium dioxide during reduction in high-pressure hydrogen, Nat. Mater. 17 (10) (2018) 923–928.
[9] S. Chen, Y.H. Hu, Color TiO2 materials as emerging catalysts for visible–NIR light photocatalysis, a review, Catal. Rev. (2023) 1–41.
[10] W.-J. Ong, L.-L. Tan, S.-P. Chai, S.-T. Yong, A.R. Mohamed, Facet-dependent photocatalytic properties of TiO2–based composites for energy conversion and environmental remediation, ChemSusChem 7 (3) (2014) 690–719.
[11] Y. Yan, M. Han, A. Konkin, T. Koppe, D. Wang, T. Andreu, G. Chen, U. Vetter, J. R. Morante, P. Schaaf, Slightly Hydrogenated TiO2 with Enhanced Photocatalytic Performance, 2014.
[12] X. Chen, L. Liu, F. Huang, Black titanium dioxide (TiO2) nanomaterials, Chem. Soc. Rev. 44 (7) (2015) 1861–1885.
[13] X. Chen, L. Liu, P.Y. Yu, S.S. Mao, Increasing solar absorption for photocatalysis with black hydrogenated titanium dioxide nanocrystals, Science 331 (6018) (2011) 746–750.
[14] T. Su, Y. Yang, Y. Na, R. Fan, L. Li, L. Wei, B. Yang, W. Cao, An in- sight into the role of oxygen vacancy in hydrogenated TiO2 nanocrystals in the performance of dye–sensitized solar cells, ACS Appl. Mater. Interfaces 7 (6) (2015) 3754–3763.
[15] A. Naldoni, M. Altomare, G. Zoppellaro, N. Liu, S. Kment, R. Zboril, P. Schmuki, Photocatalysis with reduced TiO2: from black TiO2 to cocatalyst–free hydrogen production, ACS Catal. 9 (1) (2018) 345–364.
[16] H. Choi, S.-I. Moon, T. Song, S. Kim, Hydrogen-free defects in hydrogenated black TiO2, Phys. Chem. Chem. Phys. 20 (30) (2018) 19871–19876.
[17] J. Gao, J. Zhang, W. Huang, S. Zheng, Q. Shi, Highly stable visible-light photocatalytic properties of black rutile TiO2 hydrogenated in ultrafast flow, J. Mater. Sci. Mater. Electron. 32 (2021) 14665–14676.
[18] F.G. Echeverrigaray, A.R. Zanatta, F. Alvarez, Reducible oxide and allotropic transition induced by hydrogen annealing: synthesis routes of TiO2 thin films to tailor optical response, J. Mater. Res. Technol. 12 (2021) 1623–1637.
[19] P. Rychtowski, B. Tryba, D. Baranowska, B. Zielinska, H. Nishiguchi, M. Toyoda, Hydrogen evolution on the reduced TiO2 under simulated solar lamp, Catal. Today 423 (2023) 113989.
[20] H. Liu, H. Ma, X. Li, W. Li, M. Wu, X. Bao, The enhancement of TiO2 photocatalytic activity by hydrogen thermal treatment, Chemosphere 50 (1) (2003) 39–46.
[21] H. Huang, L. Pan, C.K. Lim, H. Gong, J. Guo, M.S. Tse, O.K. Tan, Hydrothermal growth of TiO2 nanorod arrays and in situ conversion to nanotube arrays for highly efficient quantum dot-sensitized solar cells, Small 9 (18) (2013) 3153–3160.
[22] A. Baqaei, A.A.S. Alvani, H. Sameie, Enhancement of visible-light photo-activity of TiO2 arrays for environmental water purification, Pigment Resin Technol. (2022) (ahead-of-print).
[23] C. Wang, X. Kang, J. Liu, D. Wang, N. Wang, J. Chen, J. Wang, C. Tian, H. Fu, Ultrathin black TiO2 nanosheet-assembled microspheres with high stability for efficient solar–driven photocatalytic hydrogen evolution, Inorg. Chem. Front. 10 (4) (2023) 1153–1163.
[24] L. Andronic, A. Enesca, Black TiO2 synthesis by chemical reduction methods for photocatalysis applications, Front. Chem. 8 (2020) 565489.
[25] S. Tuntithavornwat, C. Saisawang, T. Ratvijitvech, A. Watthanaphanit, M. Hunsom, A.M. Kannan, Recent development of black TiO2 nanoparticles for photocatalytic H2 production: an extensive review, Int. J. Hydrogen Energy 55 (2024) 1559–1593.
[26] Y. Liang, G. Huang, X. Xin, Y. Yao, Y. Li, J. Yin, X. Li, Y. Wu, S. Gao, Black titanium dioxide nanomaterials for photocatalytic removal of pollutants: a review, J. Mater. Sci. Technol. 112 (2022) 239–262.
[27] C.-C. Wang, P.-H. Chou, Effects of various hydrogenated treatments on formation and photocatalytic activity of black TiO2 nanowire arrays, Nanotechnology 27 (32) (2016) 325401.
[28] M. Soleimani, J.B. Ghasemi, A. Badiei, Black titania; novel researches in synthesis and applications, Inorg. Chem. Commun. 135 (2022) 109092.
[29] B. Wang, S. Shen, S.S. Mao, Black TiO2 for solar hydrogen conversion, J. Materiom. 3 (2) (2017) 96–111.
[30] D. Cronemeyer, Infrared absorption of reduced rutile TiO2 single crystals, Phys. Rev. 113 (5) (1959) 1222.
[31] S. Wu, X. Li, Y. Tian, Y. Lin, Y.H. Hu, Excellent photocatalytic degradation of tetracycline over black anatase–TiO2 under visible light, Chem. Eng. J. 406 (2021) 126747.
[32] L. Zhang, T.C.A. Ng, X. Liu, Q. Gu, Y. Pang, Z. Zhang, Z. Lyu, Z. He, H.Y. Ng, J. Wang, Hydrogenated TiO2 membrane with photocatalytically enhanced anti-fouling for ultrafiltration of surface water, Appl. Catal. B Environ. 264 (2020) 118528.
[33] A.L. Valenzuela, M. Green, X. Chen, Photocatalytic degradation of antibiotics and dyes in wastewater by hydrogenated black titanium dioxide nanoparticles using design of experiment L9 taguchi orthogonal array, Gener. Chem. 7 (4) (2021) 210006.
[34] K.M. Fuentes, D. Venuti, P. Betancourt, Black titania with increased defective sites for phenol photodegradation under visible light, React. Kinet. Mech. Catal. 131 (2020) 423–435.
[35] E. Wierzbicka, M. Altomare, M. Wu, N. Liu, T. Yokosawa, D. Fehn, S. Qin, K. Meyer, T. Unruh, E. Spiecker, L. Palmisano, M. Bellardita, J. Will, P. Schmuki, Reduced grey brookite for noble metal free photocatalytic H2 evolution, J. Mater. Chem. A 9 (2021) 1168–1179.
[36] N. Denisov, S. Qin, G. Cha, J. Yoo, P. Schmuki, Photoelectrochemical properties of "increasingly dark" TiO2 nanotube arrays, J. Electroanal. Chem. 872 (2020) 114098.
[37] K.M. Chahrour, F. Yam, A. Eid, A.A. Nazeer, Enhanced photoelectro- chemical properties of hierarchical black TiO2-x nanolaces for Cr (VI) photocatalytic reduction, Int. J. Hydrogen Energy 45 (43) (2020) 22674–22690.
[38] Y. Xu, Q. Lin, R. Ahmed, E.R. Hoglund, G. Zangari, Synthesis of TiO2–based nanocomposites by anodizing and hydrogen annealing for efficient photoelectrochemical water oxidation, J. Power Sources 410 (2019) 59–68.
[39] H.Y. Yoo, M.S. Kim, H. Shin, J. Lim, Peroxymonosulfate activation by black TiO2 nanotube arrays under solar light: switching the activation mechanism and enhancing catalytic activity and stability, J. Hazard Mater. 433 (2022) 128796.
[40] Z. Wang, C. Yang, T. Lin, H. Yin, P. Chen, D. Wan, F. Xu, F. Huang, J. Lin, X. Xie, et al., H–doped black titania with very high solar absorption and excellent photocatalysis enhanced by localized surface plasmon resonance, Adv. Funct. Mater. 23 (43) (2013) 5444–5450.
[41] H.-R. An, S.Y. Park, H. Kim, C.Y. Lee, S. Choi, S.C. Lee, S. Seo, E.C. Park, Y.-K. Oh, C.-G. Song, et al., Advanced nanoporous TiO2 photocatalysts by hydrogen plasma for efficient solar–light photocatalytic application, Sci. Rep. 6 (1) (2016) 29683.
[42] S.Z. Islam, A. Reed, S. Nagpure, N. Wanninayake, J.F. Browning, J. Strzalka, D. Y. Kim, S.E. Rankin, Hydrogen incorporation by plasma treatment gives mesoporous black TiO2 thin films with visible photo- electrochemical water oxidation activity, Microporous Mesoporous Mater. 261 (2018) 35–43.
[43] X. Wang, L. Mayrhofer, M. Hoefer, S. Estrade, L. Lopez-Conesa, H. Zhou, Y. Lin, F. Peiro, Z. Fan, H. Shen, et al., Facile and efficient atomic hydrogenation enabled black TiO2 with enhanced photo–electrochemical activity via a favorably low–energy–barrier path- way, Adv. Energy Mater. 9 (33) (2019) 1900725.
[44] A. Godoy-Junior, A. Pereira, B. Damasceno, I. Horta, M. Gomes, D. Leite, W. Miyakawa, M. Baldan, M. Massi, R. Pessoa, et al., Tailoring black TiO2 thin films: insights from hollow cathode hydrogen plasma treatment duration, Plasma 6 (2) (2023) 362–378.
[45] X. Wang, L. Mayrhofer, M. Keunecke, S. Estrade, L. Lopez-Conesa, M. Moseler, A. Waag, L. Schaefer, W. Shi, X. Meng, J. Chu, Z. Fan, H. Shen, Low-energy hydrogen ions enable efficient room-temperature and rapid plasma hydrogenation of TiO2 nanorods for enhanced photoelectrochemical activity, Small 18 (2022) 2204136.
[46] M.E. Sener, R. Quesada-Cabrera, I.P. Parkin, D.J. Caruana, Facile formation of black titania films using an atmospheric–pressure plasma jet, Green Chem. 24 (6) (2022) 2499–2505.
[47] E. Khorashadizade, K. Rahimi, S. Mohajernia, S. Hejazi, N. Naseri, O. Moradlou, A. Z. Moshfegh, P. Schmuki, Comparing plasma reduction and thermal hydrogenation of TiO2 nanotubes in creating surface/bulk oxygen vacancy defects for enhanced photoelectrochemical H2 production, Bulk Oxygen Vacancy Defects for Enhanced Photoelectrochemical H2 Production.Available at SSRN: https://ssrn.com/abstract=4570075orhttps://doi.org/10.2139/ssrn.4570075.
[48] D.-H. Yoon, M.R.U.D. Biswas, A. Sakthisabarimoorthi, Impact of crystalline core/amorphous shell structured black TiO2 nanoparticles on photoelectrochemical water splitting, Opt. Mater. 133 (2022) 113030.

[49] D.-H. Yoon, M.R. Ud Dowla Biswas, A. Sakthisabarimoorthi, Enhancement of photoelectrochemical activity by Ag coating on black TiO2 nanoparticles, Mater. Chem. Phys. 291 (2022) 126675.
[50] M. Ji, E.R. Kim, M.-J. Park, H.Y. Jeon, J. Moon, J. Byun, Y.-I. Lee, Simple synthesis of black TiO 2 nanofibers via calcination in inert atmosphere, Arch. Metall. Mater. (2022) 1481–1486.
[51] G. Li, R. Huang, C. Zhu, G. Jia, S. Zhang, Q. Zhong, Effect of oxygen vacancies and its quantity on photocatalytic oxidation performance of titanium dioxide for NO removal, Colloids Surf. A Physicochem. Eng. Asp. 614 (2021) 126156.
[52] X. Zhang, M. Cai, N. Cui, G. Chen, G. Zou, L. Zhou, Defective black TiO2: effects of annealing atmospheres and urea addition on the properties and photocatalytic activities, Nanomaterials 11 (2021) 2648.
[53] J. Chen, Y. Fu, F. Sun, Z. Hu, X. Wang, T. Zhang, F. Zhang, X. Wu, H. Chen, G. Cheng, R. Zheng, Oxygen vacancies and phase tuning of self-supported black TiO2-X nanotube arrays for enhanced sodium storage, Chem. Eng. J. 400 (2020) 125784.
[54] X. Bi, G. Du, A. Kalam, D. Sun, Y. Yu, Q. Su, B. Xu, A.G. Al-Sehemi, Tuning oxygen vacancy content in TiO2 nanoparticles to enhance the photocatalytic performance, Chem. Eng. Sci. 234 (2021) 116440.
[55] L. Chen, D. Yao, H. Liang, Y. Xia, Y.-P. Zeng, Enhanced ventilation processes on vacuum thermal reduction TiO2 porous ceramics for high-efficiency solar-driven interfacial evaporation, Energy Technol. 11 (2023) 2300430.
[56] R. Katal, M. Salehi, M.H. Davood Abadi Farahani, S. Masudy-Panah, S.L. Ong, J. Hu, Preparation of a new type of black TiO2 under a vacuum atmosphere for sunlight photocatalysis, ACS Appl. Mater. Interfaces 10 (2018) 35316–35326.
[57] Y. Zhang, H. Wang, T. He, Y. Li, Y. Guo, J. Shi, Y. Xu, J. Zhang, The effects of radio frequency atmospheric pressure plasma and thermal treatment on the hydrogenation of TiO2 thin film, Plasma Sci. Technol. 25 (2023) 065504.
[58] M.I. Nandasiri, V. Shutthanandan, S. Manandhar, A.M. Schwarz, L. Oxenford, J. V. Kennedy, S. Thevuthasan, M.A. Henderson, Instability of hydrogenated TiO2, J. Phys. Chem. Lett. 6 (22) (2015) 4627–4632.
[59] N. Liu, C. Schneider, D. Freitag, E.M. Zolnhofer, K. Meyer, P. Schmuki, Noble–metal–free photocatalytic H2 generation: active and inactive 'black'TiO2 nanotubes and synergistic effects, Chem. Eur. J. 22 (39) (2016) 13810–13814.
[60] D. Zyabkin, H. Gunnlaugsson, J. Goncalves, K. Bharuth-Ram, B. QiUnzueta, D. Naidoo, R. Mantovan, H. Masenda, S. Olafsson, et al., Experimental and theoretical study of electronic and hyperfine properties of hydrogenated anatase (TiO2): defect interplay and thermal stability, J. Phys. Chem. C 124 (13) (2020) 7511–7522.
[61] J.Y. Huh, S.H. Ma, K. Kim, E.H. Choi, H.J. Lee, H.U. Lee, Y.C. Hong, et al., Facile, rapid, one-pot synthesis of hydrogenated TiO2 by using an atmospheric–pressure plasma jet submerged in solution, Scripta Mater. 162 (2019) 9–13.
[62] J. Liu, J. Yan, Q. Shi, H. Dong, J. Zhang, Z. Wang, W. Huang, B. Chen, H. Zhang, Pressure dependence of electrical conductivity of black titania hydrogenated at different temperatures, J. Phys. Chem. C 123 (7) (2019) 4094–4102.
[63] P.A.K. Reddy, P.V.L. Reddy, S.P. Vattikuti, Black TiO2: an Emerging Photocatalyst and its Applications, Nanostructured Materials for Environmental Applications, 2021, pp. 267–297.
[64] L. Liao, M. Wang, Z. Li, X. Wang, W. Zhou, Recent advances in black TiO2 nanomaterials for solar energy conversion, Nanomaterials 13 (3) (2023) 468.
[65] L. Zou, Y. Zhu, Z. Hu, X. Cao, W. Cen, Remarkably improved photo-catalytic hydrogen evolution performance of crystalline TiO2 nanobelts hydrogenated at atmospheric pressure with the assistance of hydrogen spillover, Catal. Sci. Technol. 12 (18) (2022) 5575–5585.
[66] C. Wang, C. Qian, T. Hu, X. Yang, Enhancing solar–driven photoelectrocatalytic efficiency of au nanoparticles with defect–rich hydrogenated TiO2 toward ethanol oxidation, Chem. Eng. J. 445 (2022) 136562.